

## Probing Intra-Granular Elastic Strain, Dislocation Density and Dislocation Substructure in Metallic Four Point Bend Samples

Beamline: BM32  
Proposal number: MA-938  
Beamtime allocation: 12 Feb 2010 - 16 Feb 2010 12 shifts  
Proposers: Mr. Felix Hofmann (PI)  
Dr. Sophie Eve  
Dr. Jonathan Belnoue  
Dr. Xu Song  
Prof. Alexander M. Korsunsky  
Local contact: Dr. Jean-Sébastien Micha

### Introduction:

Micro-beam Laue diffraction is a powerful technique for the probing of lattice orientation and elastic strain within individual grains of polycrystalline engineering alloys [1, 2]. A polychromatic, micro-focussed X-ray beam is used to illuminate a scattering volume smaller than the size of the crystallites. The resulting Laue single crystal diffraction patterns are recorded on an area detector and consist of a number of diffraction peaks. By indexing the peaks and refining their positions, the lattice orientation and elastic strain in the scattering volume can be determined. A map of point measurements can be built up by rastering over the sample.

Whilst lattice orientation/rotation can be readily and reliably deduced, the accurate measurement of the local deviatoric elastic strain tensor is much more challenging. This is reflected in the literature. Only few papers mention elastic strain measurements and in general the reported strains are large, e.g. in thin films [3] or metal matrix composites [4]. Approximate strain errors are estimated to be of the order of  $10^{-4}$ . There does not appear to be any systematic treatment of these errors and their sources in the literature.

The aim of this experiment was to assess the reliability with which elastic strain measurements can be performed on beamline BM32 and to quantify the experimental error sources. A particularly suitable object to study in this context is the four point bending configuration. In the central sample section pure bending exists. The total strain distribution is defined by kinematics. During elastic loading, when total equals elastic strain, this variation is linear. Beyond the elastic limit, the yield behaviour both in tension and compression can be explored [5]. To study the extremes as far as ease of elastic strain measurement is concerned, a single crystal silicon and a copper beam sample were considered. Wafer quality single crystal silicon has very low defect density. It is a near perfect crystal and at room temperature supports only elastic loading. Large copper single crystals on the other hand are easily deformed plastically and have comparatively high defect densities. They are tricky samples for accurate diffraction measurements of elastic strain.

## Experimental Setup:

The dedicated micro-beam Laue diffraction setup on BM32 was used. A schematic of the setup is shown in figure 1. Calibration of the geometrical parameters of the setup was based on diffraction patterns collected from a Germanium single crystal placed at the sample position. Consistent positioning of the sample and the reference crystals was achieved using an optical microscope with a small depth of focus mounted perpendicular to the sample surface. Line measurements of Laue patterns were collected along a line in the x-direction across the central section of the sample (figure 1). Loading was applied to the sample by displacement of the four loading rollers (A, B, C, D) in the directions of the arrows shown in figure 1. Both the load applied to the sample and the displacement of rollers B&C relative to rollers A&D in the x-direction were recorded.

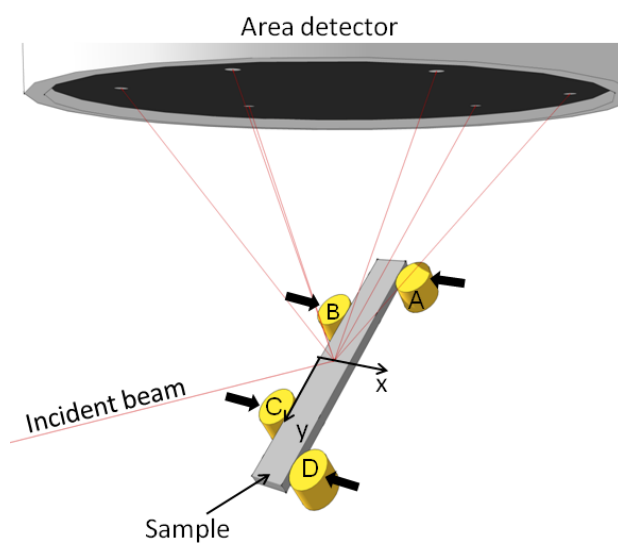


Figure 1: Schematic of the four point bending configuration used on beamline BM32.

The incident beam was pre-focussed onto a set of slits with a gap of  $20 \times 20 \mu\text{m}^2$  35m from the source. These slits act as a secondary source for the fine focussing KB optics mounted just upstream of the sample. After alignment the focal spotsize on the sample was  $0.5 \times 0.7 \mu\text{m}^2$  (FWHM). The approximate geometrical parameters of the experimental configuration are given in table 1. The detector centre was positioned at  $2\theta = 90^\circ$ .

Sample to detector distance	70mm
Photon energy range	5 - 25 keV
CCD size	$165 \times 165 \text{mm}^2$ (2048 $\times$ 2048 pixels)
Detector centre	pixels 1024 & 1024

Table 1: Approximate geometrical parameters of the experimental setup.

Ten Germanium calibration patterns were collected before and after each four point bend sample line measurement. Based on an average of these patterns, the exact geometrical parameters of the setup that should be used for the refinement of each line measurement were determined.

$\Delta x_{cent}$	$\Delta y_{cent}$	$\Delta d$	$\Delta \alpha$	$\Delta \beta$	$\Delta \gamma$
0.22 $\mu$ m	1.94 $\mu$ m	2.39 $\mu$ m	0.0024°	0.0017°	0.0011°

Table 2: Standard deviation of the geometrical parameters of the experimental setup.  $\Delta x_{cent}$  and  $\Delta y_{cent}$  are the variations of the detector centre position.  $\Delta d$ ; variation of the sample to detector distance.  $\Delta \alpha$  changes in detector roll about the incident beam.  $\Delta \beta$  variations in detector pitch about the x-axis.  $\Delta \gamma$  detector yaw variations.

By refining each Germanium reference pattern individually the random fluctuations of the geometrical parameters of the setup could be assessed (table 2). These fluctuations are due to mechanical instabilities, positioning changes due to thermal expansion and vibrations. Feeding these geometrical variations into a computational strain error estimation framework for Laue diffraction we have developed in our group, the anticipated strain error for an ideal sample can be estimated as  $\sim 40 \times 10^{-6}$ .

### Results:

A number of loading increments were applied to the Si single crystal bent beam sample. Figure 2 shows line plots of elastic strain component  $\epsilon_{yy}$  measured along a line in the x-direction across the central section of the sample at loads of 0N, 17N and 42N. As expected, since Silicon can only sustain elastic deformations at room temperature and pressure, the plots show a linear variation of  $\epsilon_{yy}$ . The strain gradients agree well with the values computed from simple beam bending theory.

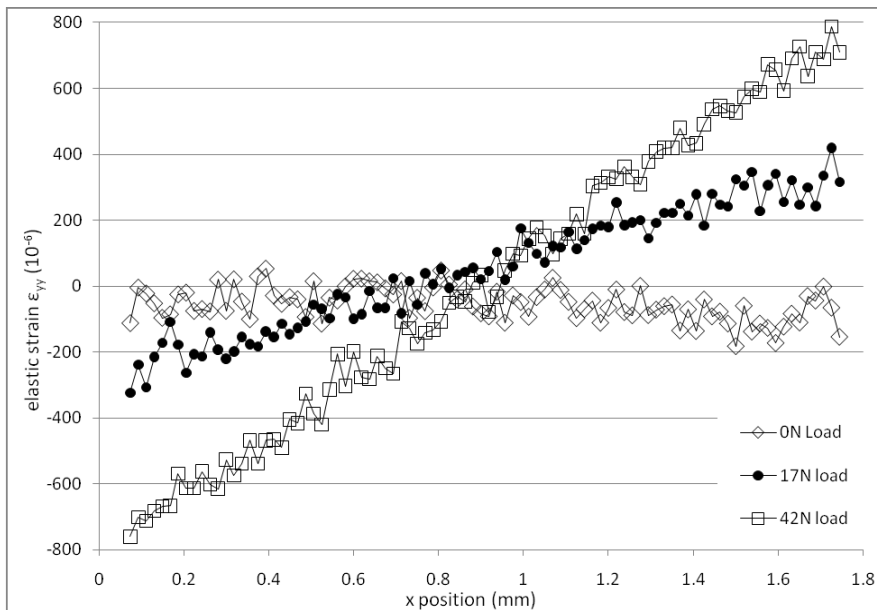


Figure 2: Profiles of elastic strain,  $\epsilon_{yy}$ , measured along a line in the x-direction across the central section of the silicon beam four point bend sample at three different applied loads.

Some noise of the strain measurement about the predicted straight line is evident. The average strain error of the measurement can be estimated as  $45 \times 10^{-6}$ . This is slightly larger than the predicted strain error based on the geometrical fluctuations of the setup. Most of this difference can be accounted for by taking into account residual pixel position errors of the X-ray camera after distortion correction.

Similar to the Silicon beam sample, a number of loading increments were also applied to the single crystal copper bar. Figure 3 shows the profile of elastic strain component  $\epsilon_{yy}$  measured along a line in the x-direction across the central section of the sample at a displacement of the loading rollers of  $80\mu\text{m}$  and a load of  $10.5\text{N}$  (grey line). This loading corresponds to the elastic limit of the copper bar sample. Clearly the elastic strain profile is much noisier than in the case of the silicon beam. The data plotted after the application of a five point moving average filter is shown superimposed (solid line). Based on the loading one would expect a linear variation of elastic strain. A straight line fitted to the  $\epsilon_{yy}$  profile is superimposed on the plot. Its gradient agrees very well with the value expected from beam bending theory. Considering the deviations of the measured profile from the straight line the average strain error can be estimated as  $320 \times 10^{-6}$ . This is significantly higher than for the single crystal silicon beam sample.

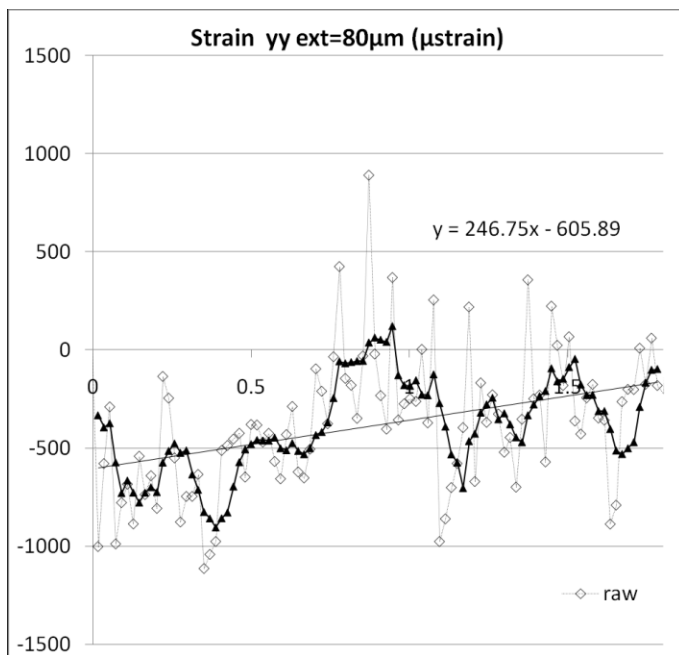


Figure 3: Profile of elastic strain,  $\epsilon_{yy}$ , measured along a line in the x-direction across the central section of the elastically deformed copper single crystal four point bend sample.

After plastic deformation to a maximum roller displacement of  $1500\mu\text{m}$ , the copper beam was unloaded and the line measurement across the central section repeated. Figure 4 shows the measured profile of stress  $\sigma_{yy}$  after unloading. It has an inverted N shaped profile. This kind of residual stress distribution is well known from powder diffraction measurements of macroscopic residual stress in polycrystalline beam samples unloaded after plastic four point bending [5]. By integrating in the x-direction, equilibrium of the sample in the y-direction can be confirmed. However the stress profile does not satisfy moment equilibrium.

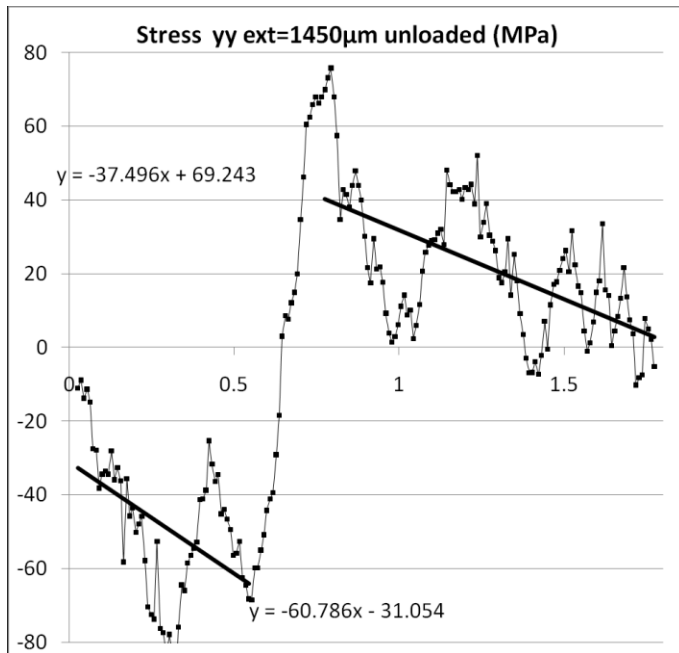


Figure 4: Profile of residual stress,  $\sigma_{yy}$ , measured along a line in the x-direction across the central section of the unloaded copper single crystal four point bend sample after plastic deformation.

The reason for the significantly larger experimental strain errors in the copper sample compared to the silicon beam sample is not immediately clear. The key difficulty appears to lie in the accurate fitting the centres of diffraction spots when even just a small amount of streaking is present. Thus far, fitting with 2D Gaussian and Lorentzian functions was tried. In both cases finding the centre of distorted diffraction peaks which is representative of the average behaviour of the scattering volume is difficult. Potential avenues for improvement would be to use more advanced fitting functions which can cope with fragmented and streaked Laue peaks, or to reduce the size of the sampling volume and the lattice orientation spread which causes Laue spot streaking and fragmentation.

#### Conclusions and Future Work:

In these measurements we determined the geometrical stability of the micro-bema Laue diffraction setup on beamline BM32. Under ideal conditions, predicted strain errors based on setup stability agree well with those found experimentally. Average strain measurement errors as low as  $45 \times 10^{-6}$  are feasible. The effect of individual error sources can be studied more closely using a computational error analysis framework we have developed. Details of this will be published elsewhere.

Under less optimal conditions, e.g. in a "soft" sample, such as the copper bar, measurement errors are significantly higher. Still, salient values, such as strain gradients, can be successfully extracted. This situation could be improved by reducing sampling volume size and hence lattice orientation spread. One way of doing this is by Differential Aperture X-ray Microscopy (DAXM), which is currently being implemented on BM32.

Given the good stability of the experimental setup on BM32 and the low strain errors which can be achieved, we plan to use this instrument to study more closely the insitu response at the grain level of individual grains within polycrystalline aggregates. In particular this will provide a direct

comparison for crystal plasticity simulations. Experimental time to study the competing inelastic deformation mechanisms by dislocation glide and twinning in Mg alloys has been scheduled for the near future.

References:

1. Hofmann, F, Song, X, Dolbnya, I, Abbey, B, and Korsunsky, A M, *Procedia Engineering*. **1(1)**: p. 193-196. (2009)
2. Ice, G E and Pang, J W L, *Materials Characterization*. **60(11)**: p. 1191-1201. (2009)
3. Budai, J D, Yang, W, Tamura, N, Chung, J-S, Tischler, J Z, Larson, B C, Ice, G E, Park, C, and Norton, D P, *Nat Mater*. **2(7)**: p. 487-492. (2003)
4. Bei, H, Barabash, R I, Ice, G E, Liu, W, Tischler, J, and George, E P, *Applied Physics Letters*. **93(7)**: p. 071904-3. (2008)
5. Korsunsky, A M, Song, X, Hofmann, F, Abbey, B, Xie, M, Connolley, T, Reinhard, C, Atwood, R C, Connor, L, and Drakopoulos, M, *Materials Letters*. **64(15)**: p. 1724-1727. (2010)

Publications arising from this experimental visit:

Publications are in progress and will be added to the ESRF database at a later date.